

# Non-invasive mineral analysis of pigments of wall paintings in the Sungseonjeon Hall

Na Ra Lee, So Jin Kim, and Dong Hyeok Moon\*

Conservation Science Division, National Research Institute of Cultural Heritage, Daejeon 34122, Republic of Korea

**ABSTRACT:** Non-destructive investigations were conducted by applying various analysis methods to investigate the production period of six wall paintings of the Sungseonjeon Hall in the royal tomb of King Suro, Historic Site No. 73 in Gimhae, South Korea. Portable microscopy and portable X-ray fluorescence analysis were performed in situ, and Raman spectroscopy and X-ray diffraction were applied to small fragments of painting layers. From microscopic observations, the size and arrangement of the mineral pigment particles used in the wall paintings were confirmed to be suitable for non-destructive analysis. Among the major elements and mineral phases detected in the wall paintings that are regarded to be earlier works (late 17th century), talc, minium with cinnabar, atacamite with botallackite, and lazurite have been detected in white, red, green, and blue specimens, respectively, confirming the use of traditional mineral pigments employed since ancient times. In contrast, in wall paintings added later (after the 19th century), anatase, minium, lavendulan with cornwallite, and lazurite were detected, along with crocoite in yellow specimens. These results indicate the existence of modern traces through synthetic pigments such as titanium white, emerald green, and chrome yellow, which were introduced by the West with the passage of time.

**Key words:** wall paintings, mineral pigment, non-invasive (non-destructive) analysis, raw material identification, mineralogical traces

Manuscript received July 26, 2022; Manuscript accepted September 28, 2022

## 1. INTRODUCTION

Since prehistoric times, humans have used materials found in the earth, such as soil, rocks, metals, and wood, in various activities and to make various products; humans have shared the knowledge of previous generations through cultural heritage. Throughout human history, from the Late Pleistocene to the Holocene/Anthropocene periods, mineral-based painting materials (pigments) have been used in paintings, makeup, architectural structures, sculptures, and the surface painting of ceramics for the purposes of coloring, decoration, and protection (Watts, 2010; Siddall, 2018). For example, a recent scientific analysis reveals that Neanderthals, who were active before modern humans, used stone tools as well as colored mineral-based soil pigments as raw materials

(Hoffman et al., 2018a, 2018b; Martí et al., 2021). Therefore, the scientific analysis of pigments in colored works of cultural heritage can have extensive geoscientific and archaeological implications, and aid in the identification of their raw materials.

According to literatures on the history of pigments, various mineral species have been used as pigment raw materials since ancient times (Barnett et al., 2006; Wagner et al., 2007; Watts, 2010; Ribechini et al., 2011; Holakooei and Karimy, 2015; Siddall, 2018; Reiche, 2019; Gliozzo and Ionescu, 2022). In the case of white pigments, minerals obtained from deposits of white earth {such as calcite [CaCO<sub>3</sub>], aragonite [CaCO<sub>3</sub>], dolomite [CaMg(CO<sub>3</sub>)<sub>2</sub>], huntite [Mg<sub>3</sub>Ca(CO<sub>3</sub>)<sub>4</sub>], and gypsum [CaSO<sub>4</sub>·2H<sub>2</sub>O], kaolin minerals (e.g., kaolinite, halloysite, and dickite; [Al<sub>2</sub>(Si<sub>2</sub>O<sub>5</sub>)(OH)<sub>4</sub>]}, and galena-based synthetic phases of naturally occurring minerals (such as anglesite [PbSO<sub>4</sub>], cerussite [PbCO<sub>3</sub>], and hydrocerussite [Pb<sub>3</sub>(CO<sub>3</sub>)<sub>2</sub>(OH)<sub>2</sub>]) have been used. Carbon black, which is composed of amorphous carbon, has mainly been used as black pigments, along with various manganese oxide and hydroxide minerals, such as cryptomelane [K(Mn<sup>4+</sup><sub>7</sub>Mn<sup>3+</sup>)O<sub>16</sub>], groutite [Mn<sup>3+</sup>O(OH)], hausmannite [Mn<sup>2+</sup>Mn<sup>3+</sup><sub>2</sub>O<sub>4</sub>], hollandite [Ba(Mn<sup>4+</sup><sub>6</sub>Mn<sup>3+</sup>)<sub>2</sub>O<sub>16</sub>], manganite [Mn<sup>3+</sup>O(OH)], nsutite [(Mn<sup>4+</sup>, Mn<sup>2+</sup>)(O,OH)<sub>2</sub>], pyrolusite [Mn<sup>4+</sup>O<sub>2</sub>], ramsdellite [Mn<sup>4+</sup>O<sub>2</sub>], romanechite

Editorial responsibility: Young Kwan Sohn

### \*Corresponding author:

Dong Hyeok Moon  
Conservation Science Division, National Research Institute of Cultural Heritage, 132 Munjiro, Daejeon 34122, Republic of Korea  
Tel: +82-42-860-9072, Fax: +82-42-860-9077,  
E-mail: moonhdh@korea.kr

©The Association of Korean Geoscience Societies and Springer 2023

[(Ba,H<sub>2</sub>O)<sub>2</sub>(Mn<sup>4+</sup>,Mn<sup>3+</sup>)<sub>5</sub>O<sub>10</sub>], and todorokite [(Na,Ca,K,Ba,Sr)<sub>1-x</sub>(Mn,Mg,Al)<sub>6</sub>O<sub>12</sub>·3-4H<sub>2</sub>O]. Moreover, the use of raw galena [PbS] and plattnerite [PbO<sub>2</sub>], a decomposition product of white lead, has also been reported. In the case of red mineral pigments, metal ore minerals, such as cinnabar [HgS], litharge [PbO], and minium [Pb<sub>3</sub>O<sub>4</sub>], have been used, along with hematite [Fe<sub>2</sub>O<sub>3</sub>]-rich reddish ochre. As yellow pigment minerals, yellowish ochre based on iron hydroxides (such as goethite [FeO(OH)], jarosite [KFe<sup>3+</sup><sub>3</sub>(SO<sub>4</sub>)<sub>2</sub>(OH)<sub>6</sub>], and natrojarosite [NaFe<sub>3</sub>(SO<sub>4</sub>)<sub>2</sub>(OH)<sub>6</sub>]), orpiment [As<sub>2</sub>S<sub>3</sub>], realgar [ $\alpha$ -As<sub>4</sub>S<sub>4</sub>], mimetite [Pb<sub>5</sub>(AsO<sub>4</sub>)<sub>3</sub>Cl], and massicot [PbO; polymorphous with litharge] have been used. For green and blue pigments, naturally occurring minerals such as malachite [Cu<sub>2</sub>(CO<sub>3</sub>)(OH)<sub>2</sub>], antlerite [Cu<sub>3</sub>(SO<sub>4</sub>)(OH)<sub>4</sub>], brochantite [Cu<sub>4</sub>(SO<sub>4</sub>)(OH)<sub>6</sub>], atacamite group minerals (atacamite, clinoatacamite, and botallackite; polymorphous of [Cu<sub>2</sub>Cl(OH)<sub>3</sub>]), tyrolite [Ca<sub>2</sub>Cu<sub>9</sub>(AsO<sub>4</sub>)<sub>4</sub>(CO<sub>3</sub>)(OH)<sub>8</sub>·11H<sub>2</sub>O], veszelyite [(Cu,Zn)<sub>2</sub>Zn(PO<sub>4</sub>)<sub>2</sub>·2H<sub>2</sub>O], azurite [Cu<sub>3</sub>(CO<sub>3</sub>)<sub>2</sub>(OH)<sub>2</sub>], and lazurite [Na<sub>6</sub>Ca<sub>2</sub>(A<sub>16</sub>Si<sub>6</sub>O<sub>24</sub>)(SO<sub>4</sub>,S,S<sub>2</sub>,S<sub>3</sub>,Cl,OH)<sub>2</sub>] have been used. Furthermore, ancient synthetic analogues such as Egyptian Green [CaSiO<sub>3</sub> + Cu glass], Egyptian Blue [CaCuSi<sub>4</sub>O<sub>10</sub>], Han blue [BaCuSi<sub>4</sub>O<sub>10</sub>], and Han purple [BaCuSi<sub>2</sub>O<sub>6</sub>] have also been used.

Since the 18th century, synthetic pigments of various colors have been produced during the rapid development of the European chemical industry. According to Clark (2002) and Oh et al. (2015), representative synthetic pigments that have been used for Korean painted cultural heritages include titanium white (after 1916; titanium dioxide compounds), zinc white (after 1834; zinc oxide compounds), chrome red (early 19th century; basic lead chromate compounds), chrome yellow (after 1809; either lead chromate or solid solutions of lead chromate and lead sulfate), Prussian blue (after 1704; exotic iron pigment based on hydrous ferriammonium ferrocyanide), ultramarine blue (after 1828; sodium aluminum sulfosilicate, which is chemically identical to the principal pigment in natural lazurite), Scheel's green (after 1775; copper compounds based on cupric hydrogen arsenite), and emerald green (after 1814; copper acetoarsenite-based compounds).

In Korean traditional painting cultural heritage, naturally occurring mineral-based pigments were mainly used; however, a trend of the original pigments being replaced with synthetic pigments has been observed in Korean colored cultural heritage toward the end of the Joseon Dynasty (Song, 2018). Furthermore, there have been cases where artificial pigments were used in the restoration and repair of architectural cultural heritage since the 1970s (Park et al., 2015). Thus, it has been difficult to confirm the exact coloration date of temple wall paintings and dancheong (Korean traditional decorative coloring on wooden buildings and artifacts) that have been conserved and repainted several times; moreover, it is also difficult to clearly distinguish between the pigments used for the restoration and the original paint

according to the times (Lee et al., 2012). Therefore, investigations through scientific analysis of colored cultural heritage requires careful and accurate identification of the colored materials, especially in conserved and repainted areas.

The application of scientific analysis to the identification and valuation of raw materials used in cultural heritage properties, especially analysis carried out non-destructively without sample collection, is in increasing demand worldwide. Since the 2000s, research on the identification of raw materials in coloring materials has been conducted on Korean painting cultural heritage, including wall paintings, mainly using portable X-ray fluorescence analyzers (Chun and Lee, 2011; Yoo et al., 2014; Ha and Lee, 2015; Lee et al., 2017, 2019, 2021a). The most popular research method used in these studies was the estimation of the raw material minerals based on the major elements detected without sampling. This method is still used as a non-destructive method of identifying raw minerals. However, recently introduced portable Raman spectroscopy and non-destructive X-ray diffraction (ND-XRD) enable more precise mineral identification based on phase structure (Abe et al., 2010; Nakai and Abe, 2012; Garcia-Guinea, 2013; Hansford, 2013; Hansford et al., 2017; Culka and Jehlička, 2019; Klisińska-Kopacz, 2019; Santos et al., 2019; Saviello et al., 2019). Therefore, the complementary application of these techniques will enable more accurate mineral identification by reducing uncertainties such as polymorphic and isomorphic phases (Miriello et al., 2018; Moon and Lee, 2019; Kostomitsopoulou Marketou et al., 2020; Secco et al., 2021).

The focus of this study is on the identification of traditional mineral pigments and their inorganic synthetic analogues in Korean colored cultural heritage using non-invasive analysis techniques. Furthermore, the suitability of these analytical techniques as in situ non-destructive investigation methods at an essential storage site, which required preservation and exhibition of cultural heritage, is assessed. As subjects suitable for this study, several wall paintings of the Sungseonjeon Hall in the Royal Tomb of King Suro in Gimhae, in which the use of pigments in the past and modern times can be distinguished with the naked eye and from documentary records, were selected.

## 2. MATERIALS AND METHODS

### 2.1. Sungseonjeon Wall Paintings

The Sungseonjeon Hall in the Royal Tomb of King Suro, Historic Site No. 73 in Gimhae, South Korea, was constructed in the 24th year of King Sukjong (1698) as a hall where the royal ancestral tablets of the king and queen of Garakguk are enshrined and ancestral rites are held. In 1792, it was reconstructed into four rooms, and in the 15th year of King Gojong (1878), when

the name of the building was changed, the Jeongjagak (T-shaped wooden shrine) was demolished and a new building was built with three rooms (Lee et al., 2020).

According to Baek (1989), a total of 55 wall paintings (61 pieces) were found during the dismantling of the Sungseonjeon Hall during the “Maintenance Construction of the Tomb of King Suro (First) and Conservation Treatment of Sungseonjeon Wall Paintings” project carried out by the Cultural Heritage Administration in the 1980s. At the time of their discovery, 10 of the 55 wall paintings were found to have been copied from 45 wall paintings from the previous period. This was determined based on a difference in the workmanship of the paintings, as well as the color and texture of the pigments. Additionally, some wall paintings were painted over or their colors were changed even at the time of construction in 1987. In particular, in the case of the wall paintings located at the bottom of the building, the wall itself was not well preserved; thus, it was judged that the wall should be newly created and painted.

In situ investigation in this study, contrary to the description of Baek (1989), revealed a total of 51 wall paintings in Sungseonjeon, located at the upper, middle, and lower parts: 18 on the north side of the building, 15 on the south side, nine on the east side, and nine on the west side. The upper part carried paintings of animals and plants in the folk-painting style; the middle part

carried paintings depicting the tales of King Suro and Empress Heo, exhibiting the characteristics of a historical site; and the lower part carried paintings of figures from the deity enshrining the tablets of King Suro and plants. In particular, in the 12 wall paintings at the bottom, the deity was depicted as standing symmetrically, wearing official robes and facing the mortuary tablet of King Suro. Of these, four wall paintings on the east side and four on the north side were presumed to have been newly painted. Non-destructive analysis of these paintings are required to evaluate and preserve the Sungseonjeon wall paintings as cultural heritage.

To distinguish between the original and new materials used as mineral pigments in the Sungseonjeon wall paintings, six paintings of a deity wearing a blue robe at the bottom, similar in color and subject, were selected for the study (Fig. 1). Of these, three wall paintings were presumed to have been painted in the early period and were labeled as group O (O1, O2, and O3), and three wall paintings were presumed to have been painted later and were labeled as group N (N1, N2, and N3).

## 2.2. Investigation Points and Sample Collection

After checking the overall condition of the selected wall paintings, investigation points were selected, focusing on main



**Fig. 1.** Analysis points of Sungseonjeon wall paintings. (a) O1, (b) O2, (c) O3, (d) N1, (e) N2, and (f) N3. The red labels indicate the delaminated specimen collection points.

colors such as black, red, blue, white, green, and yellow. The labeled points in Figure 1 indicate the points for portable microscopic observation and portable X-ray fluorescence (PXRF) analysis; the red points denote the delaminated specimen collection sites.

In consideration of artistic and historic value and conservation, only very small specimens were collected from naturally peeled areas. Specimen collection was performed by separating the weakly attached remaining edge of the mural screen using tweezers, resulting in fragments approximately 5 mm in diameter. The amount of the collected specimens was approximately 10 mg on average, ranging from 2 to 30 mg depending on the volume of basecoat collected.

### 2.3. Analytical Methods

For in-field investigation, portable microscopy and PXRF were performed. The surface of the colored layer was observed using a portable microscope (Scalar, DG-3x, Japan) to determine the shape, size, and coloration of the pigment particles. The chemical composition of the coloring material was determined using a PXRF analyzer (Bruker, Tracer 5i, DEU) at the site where the wall painting was preserved using a Rh target, with operating parameters of 15–50 kV and 4.5–195 mA, the Geo Exploration mode, a spot size of 8 mm, and measuring time of 40 s.

Raman spectroscopy and XRD analyses were performed non-invasively to confirm the mineral composition of the small fragments collected at the site. These analyses used unpowdered raw specimens to examine the applicability of non-destructive in situ investigation methods.

Micro-Raman spectra were obtained using an XperRam F2.8

Raman micro spectrometer (Nanobase, Republic of Korea). A BX41M-LED microscope (Olympus, Japan) with a magnification of x40 was used to focus the laser onto the specimens. Laser wavelengths of 473 nm (2300 gr/mm) or 633 nm (1800 gr/mm) were used for excitation and the better spectrum selected based on the signal-to-background fluorescence ratio. Wavenumber calibration was performed using the Raman peak of a silicon crystal at  $520\text{ cm}^{-1}$ .

For XRD analysis, an EMPYREAN X-ray diffractometer (PANalytical Co., Netherlands) was used to continuously scan the  $2\theta$  range of  $5\text{--}60^\circ$  using a Cu target ( $\text{CuK}\alpha = 1.5406\text{ \AA}$ ), step size of  $2\theta = 0.02^\circ$ , and operating conditions of 45 kV/40 mA. Furthermore, non-destructive scanning was performed after detaching the stage for powder samples and placing the colored surface of a small specimen collected in the field in the space between the X-ray tube and the detector, as suggested by Moon and Lee (2019). This method was applied considering the equipment specifications for the position of the specimen, flatness of the analysis target surface, and scan area.

## 3. RESULTS AND DISCUSSION

### 3.1. In Situ Site Investigation

#### 3.1.1. Microscopic observation

To accurately identify the pigments painted on murals, understanding their condition in the colored layer is critical. Figures 2 and 3 show the residual status of the pigment particles in the colored layers of the group O and group N wall paintings in Sungseonjeon Hall, respectively, observed in the field using a

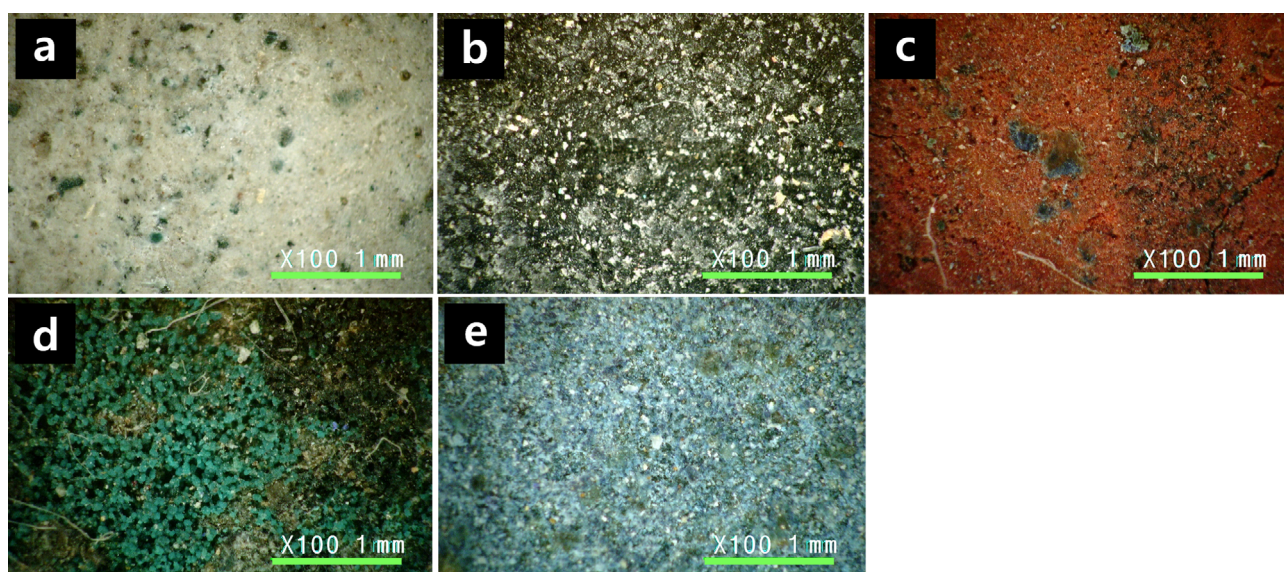


**Fig. 2.** Optical microscope images of wall painting surfaces in group O. (a) O2-W3, (b) O2-Bk2, (c) O1-R2, (d) O1-G2, and (e) O2-B2. The name of each specimen indicates the wall painting number and analysis point in Figure 1.

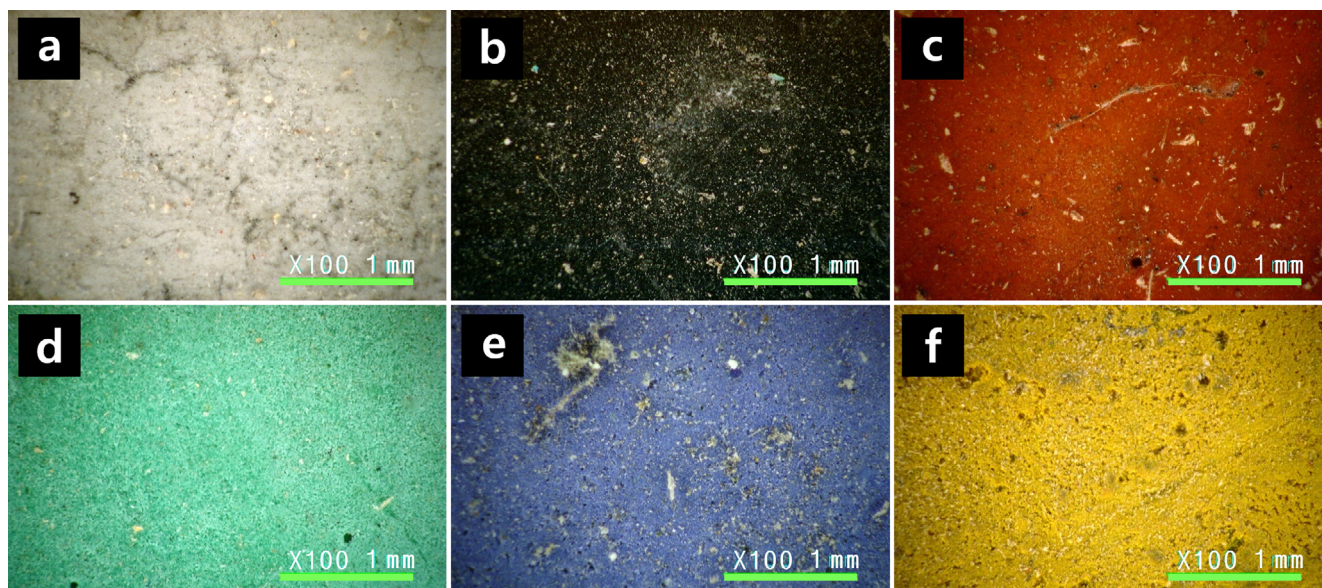


**Fig. 3.** Optical microscope images of wall painting surfaces in group N. (a) N2-W9, (b) N2-Bk5, (c) N2-R9, (d) N1-G5, (e) N2-B5, and (f) N3-Y3. The name of each specimen indicates the wall painting number and analysis point in Figure 1.

portable microscope.

In general, the pigments seemed to have been processed to a relatively smaller and more homogeneous particle size in group N than in group O. In both groups, the distinction of the colored material between the surface and lower layers was clear, with no obvious impurities (Figs. 2 and 3). In particular, the particle size and arrangement observed in Figures 2 and 3 are similar to those of randomly oriented powder pigment specimens. These conditions are suitable for the application of Raman spectroscopy and XRD as analytical methods, which can identify mineral species more directly and precisely, in addition to PXRF, which is mainly used for non-destructive in situ investigations of cultural heritage. These methods can be used to analyze raw specimens that have not undergone destructive treatment (Moon and Lee, 2019; Moon, 2021).

### 3.1.2. X-ray fluorescence analysis

Table 1 lists the major and minor elements of each color detected in the colored layers of the six wall paintings investigated. In group O, Mg and Pb were detected as main components in white pigments, and no specific element was detected in black and blue pigments. In red pigments, mainly Pb and Hg were detected, but in the case of orangish O3-R6, only Pb was detected. In green pigments, Cu and Cl were identified as the main elements, and in O3-G4, which had a bluish color compared to the other green spots, As was detected along with Cu.

In the wall paintings of group N, Ti and Pb were detected as the major elements in white and red pigments, respectively. In addition, mainly Cu and As were detected in green pigments,

and mainly Cr and Pb were detected in yellow pigments. In black and blue pigments of group N, no specific coloring element was detected for each color were relatively consistent with those of the paintings of group O.

In the case of group O, Mg-rich white earth (such as periclase [MgO] and magnesite [MgCO<sub>3</sub>], which are secondary decomposed phases of huntite, along with huntite and talc [Mg<sub>3</sub>Si<sub>4</sub>O<sub>10</sub>(OH)<sub>2</sub>]), lead white (such as anglesite, cerussite, and hydrocerussite), cinnabar, minium, and copper chlorides (such as atacamite group minerals) can be potential chromophores. The painting materials that can be identified based on PXRF data of the wall paintings in group N include titanium dioxide compounds, minium, Cu- and As-containing green mineral (such as tyrolite) or green synthetic pigments (such as Scheel's green and emerald green), and chrome yellow or yellow lead-containing minerals (such as mimetite and massicot).

However, although PXRF provides traces of specific chromophores, a wide range of potential candidates, as in the above cases, can sometimes lead to misinterpretation of painting materials. Furthermore, considering the characteristics of the equipment, thorough interpretation is required in cases of complex analyzing data detected. This is because, depending on the analysis target, interfering data can be detected from the under layer (Chun and Lee, 2011). In addition, pigments are possibly composed of elements that are beyond the detection limit of the equipment. For example, in previous non-destructive investigations of cultural heritages using PXRF, in the case of the indicator element was not detected, such as Mn-containing black minerals, it has been considered to be meok (ink stick) or carbon black, but cross-

**Table 1.** Chemical compositions of painted layers on Sungseonjeon wall paintings obtained using a portable X-ray fluorescence (PXRF) analyzer. Major and minor elements were classified by values and count rates of the PXRF spectral peaks, respectively

Painting	Investigation point	Pigment color	Major elements	Minor elements
O1	W1	White	Mg, Pb	Si, S, P, Fe, Ca
	W2	White	Pb, Mg	Si, Fe, Ca
	Bk1	Black	–	Si, Fe, Ca, S, Al, K, Mg
	R1	Red	Pb, Hg	Si, S, Mg, Ca
	R2	Red	Pb, S, Hg	Si
	G1	Green	Cu, Cl, As	Si, Mg, Al
	G2	Green	Cu, Cl	Si, Fe, Al
	B1	Blue	–	Si, S, Al, Mg, Fe
O2	W3	White	Mg, Pb	Si, S, P, Fe, Ca
	W4	White	Pb, Mg	Si, P, Fe, Ca
	Bk2	Black	–	Si, Fe, Ca, P, Mg, Al, K
	R3	Red	Pb	Si
	R4	Red	Pb, Hg	S, Si, Mg
	B2	Blue	–	Si, Al, Fe, P, K, Ca, S
O3	W5	White	Mg, Pb	Si, S, P, Fe, Ca
	W6	White	Pb, Mg	Si, P, Ca, Fe
	Bk3	Black	–	Si, Fe, Ca, P, K, Al
	R5	Red	Pb, Hg	Si, S, Al
	R6	Red	Pb	Si, S, Fe, Al, P
	G3	Green	Cu, Cl	Si, Al, Fe, P
	G4	Green	Cu, As	Mg, Si, Fe, Ca
	B3	Blue	–	Si, Al, S, Fe, Mg, P, Ca
N1	W7	White	Ti	S, Ca, Mg, Al
	W8	White	Ti	Ca, S, Mg
	Bk4	Black	–	Ca, S, Mg, Si, P, Al
	R7	Red	Pb	S, Si, Ca
	Y1	Yellow	Cr, Pb	S, Ca, Si
	G5	Green	Cu, As	Mg, Ca
	B4	Blue	–	Si, S, Al, K, Ca, P
	N2	W9	White	Ti
W10		White	Ti	Ca, Mg, S
Bk5		Black	–	Ca, S, Si, Mg, P
R8		Red	Pb	S, Si, Ca
R9		Red	Pb	Ca, Si, Cl
Y2		Yellow	Cr, Pb	S, Ca, Si
G6		Green	Cu, As	Mg, Ca
B5		Blue	–	Ti, Si, S, Al, Ca, K
N3	W11	White	Ti	Ca, S, Al, Si
	W12	White	Ti	Ca, S, Al, Si
	Bk6	Black	–	S, Ca, Mg, K
	R10	Red	Pb	S, Si
	Y3	Yellow	Cr, Pb	Si, Ca, Al
	G7	Green	Cu, As	Mg, Ca, Si
	B6	Blue	–	Si, S, Ca, K

verification for presence of amorphous carbon has not been performed (Ha and Lee, 2015; Lee et al., 2017; Alberghina et al.,

2020; Merkaç and Civici, 2020). Therefore, for the more accurate identification of minerals in pigments, it is necessary to confirm various possibilities by cross-validating analyses, such as direct mineral composition based on phase structure.

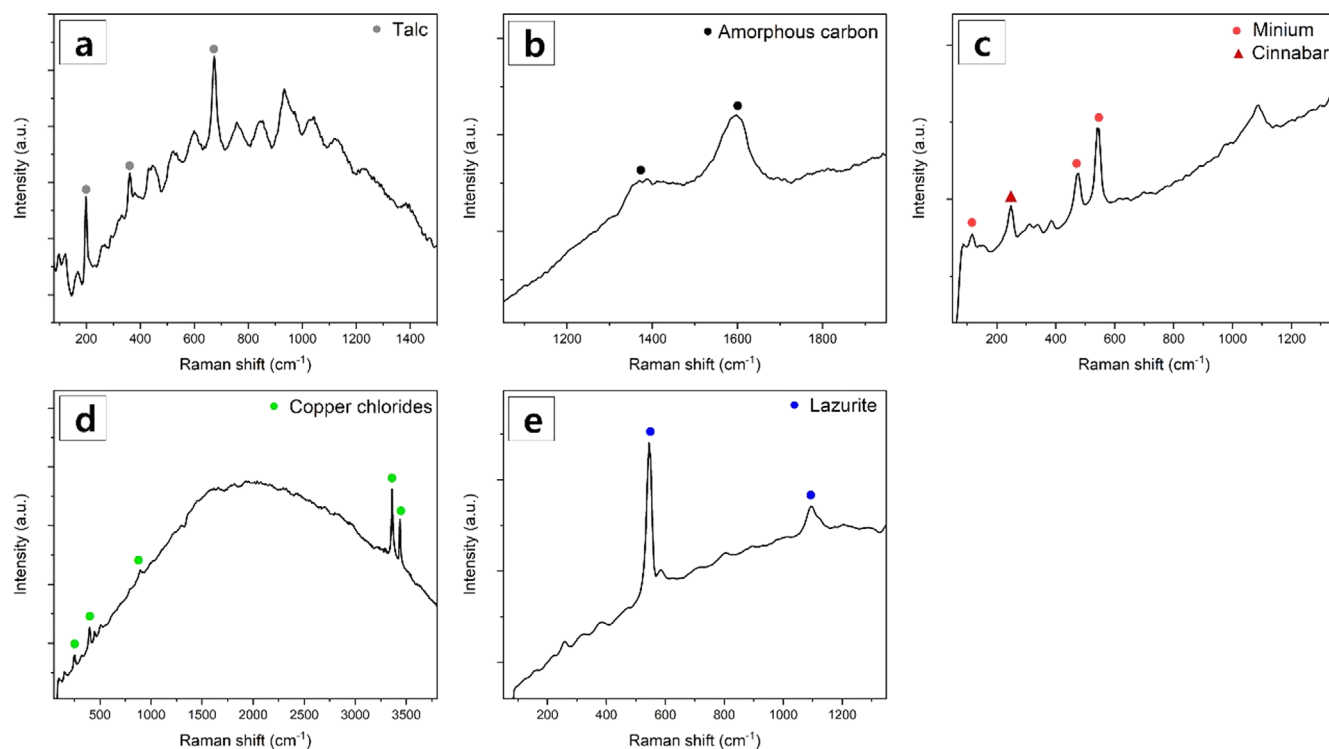
## 3.2. Non-invasive Specimen Analyses

### 3.2.1. Micro-Raman spectroscopy

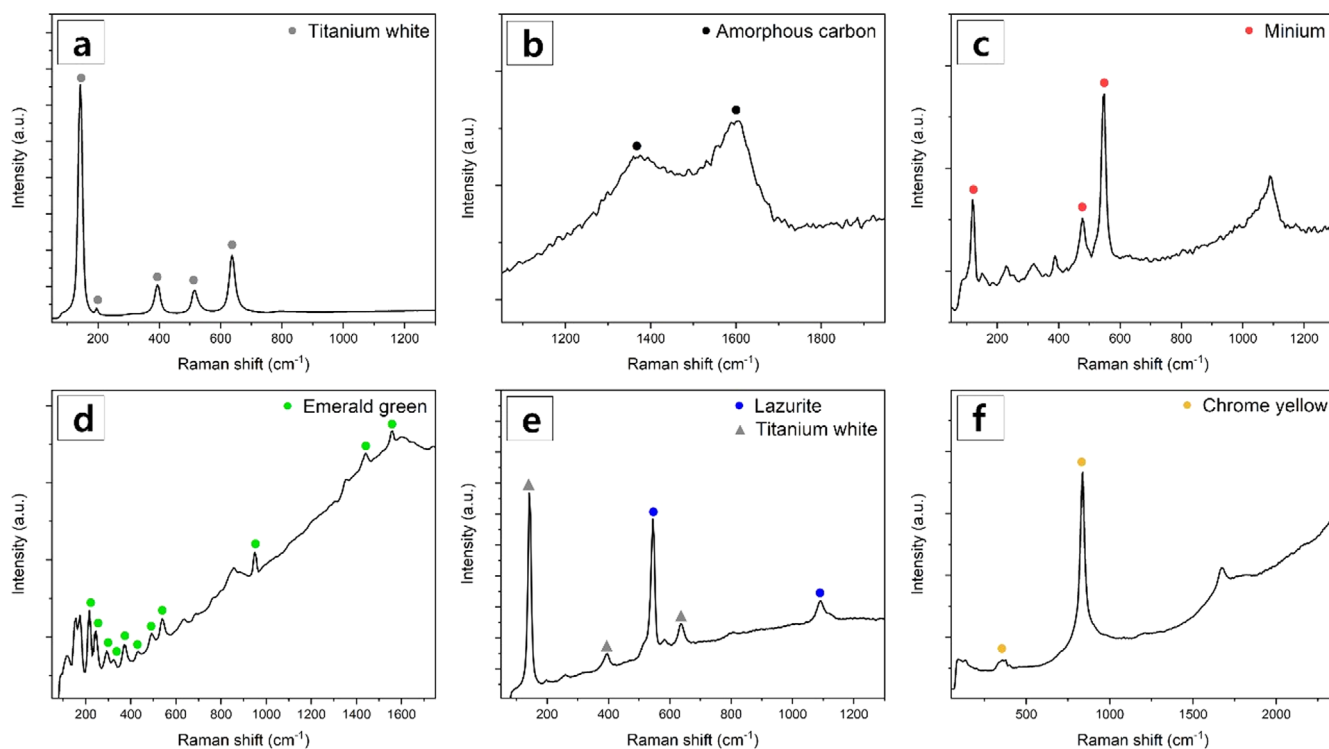
Raman spectroscopy was performed on the small fragments collected during the in situ investigation to confirm the raw materials in the pigment used in the colored layer for each color. Figure 4 shows the Raman spectrum of each colored sample collected from the group O wall paintings. The spectrum for O2-W3, a white specimen, contained noise from fluorescence, but was identified as that of talc based on peaks at 199, 361, and 674  $\text{cm}^{-1}$  (Wang et al., 2015). The broad signal from 1370 to 1594  $\text{cm}^{-1}$  identified in the spectrum of the black specimen (O2-Bk2) was considered to be related to the bands of amorphous carbon appearing widely in the areas around 1350  $\text{cm}^{-1}$  and 1600  $\text{cm}^{-1}$  (Bell et al., 1997; Tomasini et al., 2012, 2015; Gutiérrez-Neira et al., 2013). In the spectrum of the red specimen (O1-R2), the characteristic peaks of minium were confirmed at 116, 477, and 547  $\text{cm}^{-1}$  along with the characteristic peak of cinnabar at 248  $\text{cm}^{-1}$  (Bell et al., 1997; Caggiani et al., 2016; Marucci et al., 2018). The spectrum of the green specimen (O1-G2) was confirmed to contain characteristic peaks of copper chloride minerals (one of the possible isomers of atacamite, paratacamite, clinoatacamite, or botallackite) at 153, 447, 507, 896, 3307, 3376, and 3454  $\text{cm}^{-1}$  (Bertolotti et al., 2011; Coccato et al., 2016; Fan et al., 2020). The spectrum of the blue O2-B2 specimen was confirmed to contain characteristic peaks of lazurite at 545 and 1094  $\text{cm}^{-1}$  (Bell et al., 1997; Ballirano and Maras, 2006).

Figure 5 shows the Raman spectrum of each colored specimen collected from the group N wall paintings. The spectrum of the white specimen (N2-W9) exhibited characteristic peaks of anatase at 142, 195, 393, 512, and 637  $\text{cm}^{-1}$  (Lubas et al., 2014; El-Deen et al., 2018; Tuschel, 2019). The black specimen (N2-Bk5) exhibited a spectrum of amorphous carbon in a similar range as that of O2-Bk2. The spectrum of the red specimen (N2-R9) was confirmed to contain characteristic peaks of minium at 120, 120, 478, and 549  $\text{cm}^{-1}$ , and that of the green specimen (N1-G5) was confirmed to contain characteristic peaks of emerald green ( $[\text{Cu}(\text{C}_2\text{H}_3\text{O}_2)_2 \cdot 3\text{Cu}(\text{AsO}_2)_2]$ ) at 216, 247, 294, 373, 432, 490, 540, 950, 1439, and 1557  $\text{cm}^{-1}$ . Features attributable to the acetate group were evident at 950 and 1439  $\text{cm}^{-1}$ , corresponding to C–C and  $-\text{CO}_2$  stretching, respectively (Bell et al., 1997; Rosi et al., 2004; Li et al., 2020). The spectrum of the blue specimen (N2-B5) exhibited characteristic peaks of lazurite at 545 and 1092  $\text{cm}^{-1}$  and characteristic peaks of anatase at 141, 392, and 637  $\text{cm}^{-1}$ .

The yellow pigment observed only in group N was identified as chrome yellow, with its the spectrum of specimen N3-Y3 exhibiting its characteristic peaks at 355 and 839  $\text{cm}^{-1}$  (Bell et al., 1997; Caggiani et al., 2016; Papiaka et al., 2016; Geldof et al., 2019). Raman spectroscopy provides information regarding the molecular structure of the colored particles in pigments. In particular,



**Fig. 4.** Raman spectra of pigment particles in the wall paintings of group O. (a) O2-W3, (b) O2-Bk2, (c) O1-R2, (d) O1-G2, and (e) O2-B2. The name of each specimen indicates the wall painting number and analysis point in Figure 1.

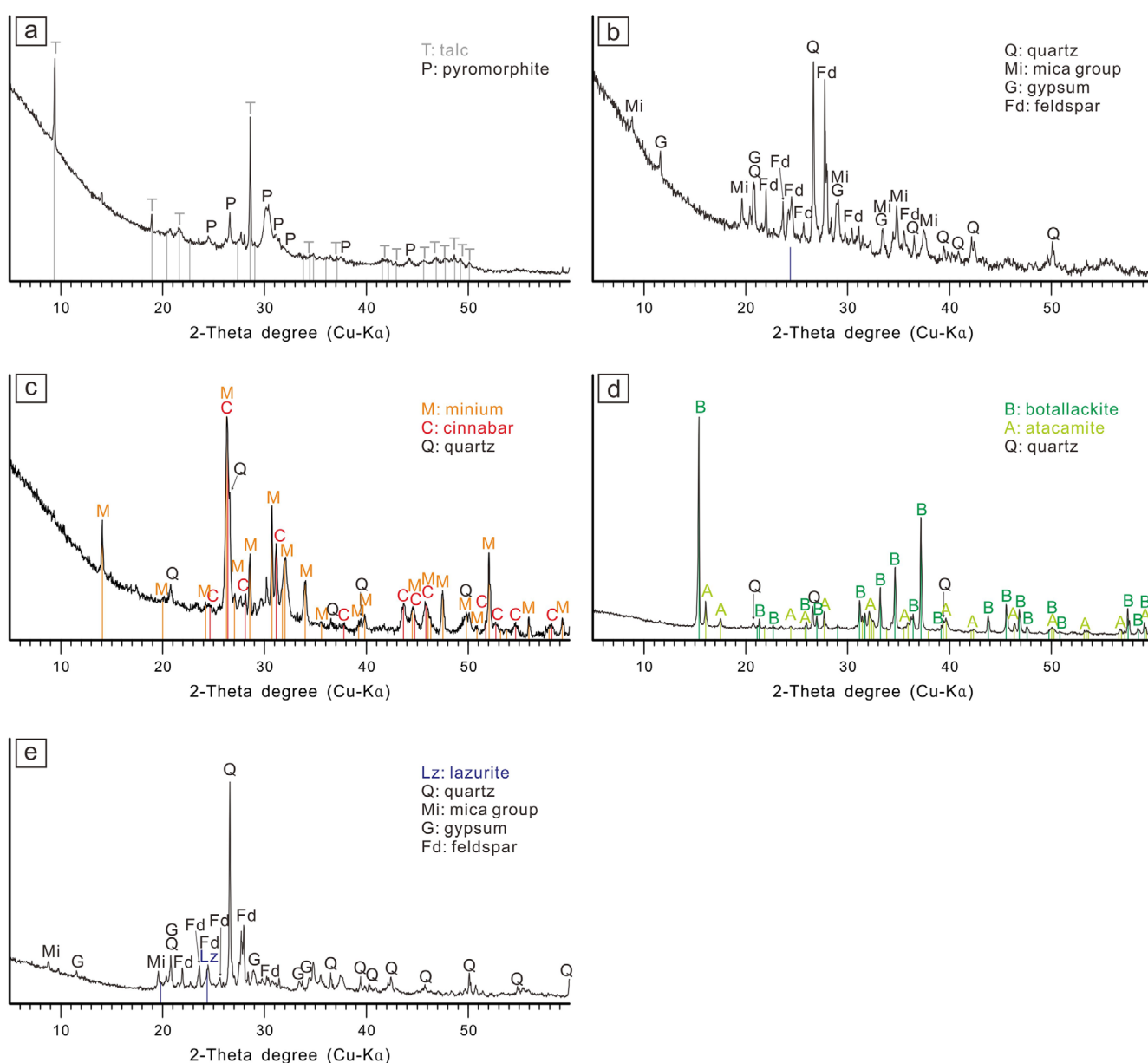


**Fig. 5.** Raman spectra of pigment particles in the wall paintings of group N. (a) N2-W9, (b) N2-Bk5, (c) N2-R9, (d) N1-G5, (e) N2-B5, and (f) N3-Y3. The name of each specimen indicates the wall painting number and analysis point in Figure 1.

characteristic peaks of amorphous carbon and lazurite were detected in the spectra of the black and blue pigments, respectively, which were not confirmed by PXRF. These results indicate that Raman spectroscopy supplemented the existing in situ investigation. However, this method may sometimes require specific mineral phase identification by cross-checking with XRD analysis (Čermáková et al., 2015; Moon et al., 2021; Shen and Shen, 2021). Examples from the present study include O2-W3 with no Pb-containing minerals, which was detected by PXRF, O1-G2 broadly identified as comprising copper chlorides, and N1-G5 and N3-Y3 containing emerald green and chrome yellow, respectively.

### 3.2.2. Non-destructive X-ray diffractometry

Figure 6 shows the XRD results of the small fragments collected from group O wall paintings. The pattern of the white specimen (O2-W3) was characterized by clear peaks of talc, along with minor diffraction peaks of pyromorphite. The diffractogram of the red specimen (O1-R2) mainly consisted of minium and cinnabar, with a small trace of quartz. The pattern of the green specimen (O1-G2) was characterized by the presence of copper chloride minerals, specifically botallackite and atacamite, with a small trace of quartz. The pattern of specimen O2-B2 was characterized by peaks of quartz, feldspar, mica, and gypsum, as well as a characteristic peak of lazurite, a blue mineral.



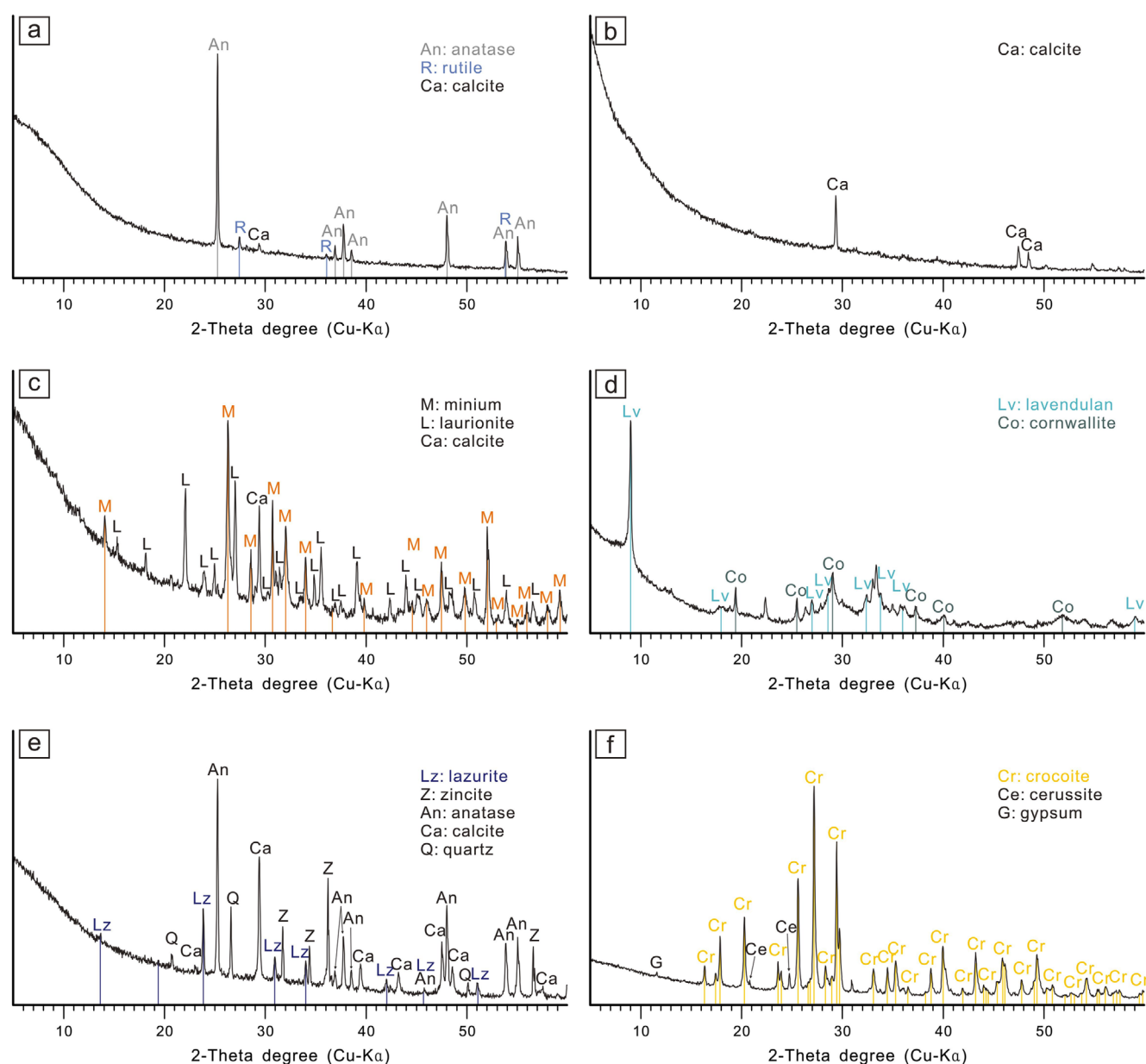
**Fig. 6.** Non-destructive X-ray diffraction results of Sungseonjeon wall painting fragments in group O. (a) O2-W3, (b) O2-Bk2, (c) O1-R2, (d) O1-G2, and (e) O2-B2. The name of each specimen indicates the wall painting number and analysis point in Figure 1.



Figure 7 shows the XRD results of the small fragments from group N wall paintings. In the pattern of the white specimen (N2-W9), the diffraction peak of anatase was dominant, and fine rutile and calcite peaks were confirmed. The diffractogram of the red pigment (N2-R9) exhibited diffraction peaks indicating a mixture of minium, laurionite, and calcite, and that of the green pigment (N1-G5) showed traces of cornwallite along with lavendulan. The pattern of N2-B5 exhibited peaks for white minerals such as zincite, anatase, calcite, and quartz, together with lazurite. The pattern of the yellow specimen (N3-Y3) exhibited peaks of crocoite, a lead chromate mineral, as a coloring mineral, along with traces of cerussite and gypsum.

The black specimens, O2-Bk2 and N2-Bk5, the diffraction patterns of black mineral species were not recorded. However, the Raman spectra in Figures 4 and 5 confirm that these black materials consisted of amorphous carbon. Therefore, amorphous carbon in the black pigment of these two specimens suggest that was not present in a sufficient amount, thickness, or crystallinity to record a X-ray halo pattern (Peng et al., 1993; Moon and Lee, 2019; Lee et al., 2021b).

The diffraction information was detected not only for the target particle but also for all particles in the scan area due to the nature of the XRD analysis. In addition to the detection of specific coloring minerals, it is suggested that additional minerals are



**Fig. 7.** Non-destructive X-ray diffraction results of Sungseonjeon wall painting fragments in group N. (a) N2-W9, (b) N2-Bk5, (c) N2-R9, (d) N1-G5, (e) N2-B5, and (f) N3-Y3. The name of each specimen indicates the wall painting number and analysis point in Figure 1.

impurities that were present in the raw materials or added as fillers, such as quartz, feldspar, and mica in group O, and calcite, gypsum, zincite, and quartz in group N. Moreover, these secondary minerals may be present in the raw materials constituting the basecoat. However, it has been noted in previous applications of ND-XRD to painted layers that mainly the diffraction patterns of mineral phases in the surface layer were recorded (Moon and Lee, 2019; Moon, 2021). To further explore these phenomena, it is necessary to observe the cross-sections of the specimens; however, because this study concerns the application of non-destructive in-field analysis of cultural heritages (Chiari, 2008; Abe et al., 2010; Nakai and Abe, 2012; Santos et al., 2019), and the specimens must be preserved, this was not feasible.

### 3.3. Raw Minerals of Pigments

For the accurate mineral identification of colored pigments in the Sungseonjeon wall paintings, we applied non-invasive Raman spectroscopy and ND-XRD analyses which can be used in future field investigations along with widely used PXRF. The raw materials for each coloring pigments identified by cross-checking the results of the three analysis techniques are discussed below. In addition, the history of each is reviewed to better convey the differences in the raw materials based on their production periods.

#### 3.3.1. White pigments

In group O, talc seems to have been mainly used as a white coloring material, possibly mixed with some Pb minerals. In group N, the synthetic pigment titanium white, which comprises titanium dioxide minerals, seems to have been used as a white coloring material.

Cases of mixing talc and Pb minerals in Korean colored cultural heritage properties have been reported not only in wall paintings but also in large Buddhist paintings (Gwaebul) (Lee et al., 2017, 2019), which have been found to contain lead carbonates, cerussite [PbCO<sub>3</sub>], and hydrocerussite [2PbCO<sub>3</sub>·Pb(OH)<sub>2</sub>]. In contrast, the Pb component detected in this study was confirmed to be that of pyromorphite [Pb<sub>5</sub>(PO<sub>4</sub>)<sub>3</sub>Cl] based on the XRD pattern (Table 1, Fig. 6), which is a mineral that rarely occurs as white in nature but is primarily green or yellowish green (Keim and Markl, 2015). It was not clear whether it was mixed with talc during the initial coloring. However, as a phase that was relatively easily decomposed from several secondary phases such as cerussite and anglesite [PbSO<sub>4</sub>] generated from the weathering of galena (Maneck et al., 2020; Gliozzo and Ionescu, 2022; Li et al., 2022), it was presumed to be a secondary phase generated from lead white added during the creation of the Sungseonjeon wall paintings.

Typical titanium dioxide phases produced in nature include

rutile, anatase, and brookite. Their crystals are reddish to yellowish brown, dark blue, gray, and black in color with a steely luster, but the streak color is a very bright shade of white, enabling the mass production of a white pigment called titanium white or Pigment White 6 (PW6) since 1916 (Clair, 2016). The pigment used in the white color of the group N Sungseonjeon wall painting analyzed in this study had the crystal structure of anatase (Figs. 5 and 7). In South Korea, titanium white has a short history of being introduced and used; it has been popularly used as a replacement for existing white pigments as it offers excellent whiteness, waterproofness, and durability (Gettens and Stout, 1942; Jeong, 2001).

#### 3.3.2. Black pigments

No component related to color was detected in the chemical composition of all the black analysis points of the two groups or in the XRD results of the specimens (Table 1, Figs. 6 and 7). However, amorphous carbon was identified in the Raman spectroscopy results of the black specimens (Figs. 4 and 5).

From these findings, the black color used in the Sungseonjeon wall paintings was mainly an amorphous carbon-based pigment called carbon black. Carbon black has traditionally been produced from carbonized organic materials (soot and chars) and has been used for a long time, from the artistic activities of prehistoric humans to the preparation of raw materials for modern paints and inks (Zilhão et al., 2010; Siddall, 2018). Considering the production period of the Sungseonjeon wall paintings, ink sticks or Chinese ink (mainly used in Asian cultures) may have been used as carbon black materials. Further, modern carbon black products with relatively improved color and durability may have been used in the production of the group N wall paintings.

#### 3.3.3. Red pigments

In group O, the red color used was created by mixing cinnabar [HgS], which was sometimes referred to as vermilion, and the lead oxide mineral minium [Pb<sub>3</sub>O<sub>4</sub>], also called red lead. In group N, only minium seems to have been used as a coloring material. Records of processing and using powders of these minerals in pigments date back to approximately 8,000 BC. As coloring materials with vivid and strong red or reddish orange hues, they have been used in various fields to date (Edwards et al., 1999; Barnett et al., 2006; Hazen et al., 2012; Clair, 2016). Therefore, the detection of these minerals was not a suitable metric to determine the production period of the Sungseonjeon wall paintings. However, sufficient sample collection for these minerals containing high concentrations of lead is expected to allow the analysis of the raw material origins based on lead isotope research in the future (Nord et al., 2015; Rodriguez et al., 2020).

### 3.3.4. Green pigments

Phases such as botallackite and atacamite were found in the green pigment of group O among the polymorphs of  $\text{Cu}_2(\text{OH})_3\text{Cl}$ , confirming that copper chloride minerals were used as a coloring material. In contrast, in the green pigment of group N, lavendulan [ $\text{NaCaCu}_5(\text{AsO}_4)_4\text{Cl}\cdot 5\text{H}_2\text{O}$ ] and cornwallite [ $\text{Cu}_5(\text{AsO}_4)_2(\text{OH})_4$ ] were detected, suggesting the use of a copper arsenate-based pigment.

Copper chloride minerals have been mainly detected in the degeneration of copper ores such as malachite and azurite and corrosive substances of copper and bronze cultural heritage artifacts (Riederer, 1974; Pollard et al., 1989; Siddall, 2018). They have been used as a popular pigment since being synthesized by the 12th century artist Theophilus, who named the copper chloride pigment “viride salsum,” meaning salt green (Eastaugh et al., 2004; Siddall, 2018). Among the copper arsenate minerals detected in the green pigment of group N, lavendulan, in particular, has been reported as a secondary phase of emerald green [ $\text{Cu}(\text{C}_2\text{H}_3\text{O}_2)_2\cdot 3\text{Cu}(\text{AsO}_2)_2$ ]; it is a synthetic pigment produced after the 19th century, formed by various reactions with the surrounding environment (Li et al., 2020). These examples indicate that the green color of group N was obtained by using more modern coloring materials compared to those of group O.

### 3.3.5. Blue pigments

For the blue painted surface, the blue pigment lapis lazuli was used for both groups O and N, because lazurite [ $\text{Na}_7\text{Ca}(\text{Al}_6\text{Si}_6\text{O}_{24})(\text{SO}_4)(\text{S}_3)\cdot \text{H}_2\text{O}$ ] was detected. Lapis lazuli occurs as a rock and has been mainly found in the jewelry of ancient civilizations such as Mesopotamia (around 7,000 years BC) and Egypt (4,000–3,500 BC). Its processing in a more refined form from the ore and use as a blue pigment has been recorded since the 6th century AD (Bicchieri, 2014; Frison and Brun, 2016; Siddall, 2018). The modern pigment synthesized from high-purity lazurite is called ultramarine blue, the production process for which was first introduced in 1828 (Kendrick et al., 2004). The blue pigment based on lazurite has been used since before the production period of the Sungseonjeon wall paintings, even in Korean colored cultural heritage properties (Kim et al., 2014; Lee et al., 2017). However, based on the non-destructive analytical method employed in this study, it is not possible to confirm whether the lapis lazuli has been purified from the ore or ultramarine blue. Therefore, this aspect needs to be addressed in future research.

### 3.3.6. Yellow pigments

The yellow pigment was used only in group N wall paintings, and was mainly composed of crocoite [ $\text{PbCrO}_4$ ], as confirmed by the detection of Cr and Pb in the PXRF results. Cases of using the natural mineral crocoite as a coloring material for yellow are

rare but have been reported in literature on ancient Egypt and some 13th century European wall paintings (Edwards et al., 2004; Mugnaini et al., 2006; Hradil et al., 2014). However, the first record of Cr-based pigments synthesized to possess a vivid yellow tint compared to natural crocoite, which was produced as a crystal with a strong red or orangish red hue, dates to 1804 or 1809. A patent for chrome yellow as a material for painting and leather tanning was registered in 1884 by Augustus Schultz and Martin Dennis (Gliozzo and Ionescu, 2022). A trend of the original pigments being replaced with synthetic pigments is observed in Korean colored cultural heritage toward the end of the Joseon Dynasty (Song, 2018), and lead chromate has been detected in recently preserved cultural heritage properties (Hong and Lee, 2013), suggesting that the use of chrome yellow as a yellow pigment was common at the time of creating the group N wall paintings in Sungseonjeon Hall.

## 3.4. Mineralogical Traces of the Period

We have identified the mineral raw materials of the pigments for each color used in six murals of Sungseonjeon via non-destructive elemental and mineral phase analyses. Based on our results, it is possible to present significant evidence for differences in the coloring materials used for early (group O) and newly added (group N) wall paintings. In particular, the detection of synthetic pigments such as titanium white, emerald green, and chrome yellow in the group N paintings indicates a production period after the end of the Joseon Dynasty (late 19th century to early 20th century) when they were broadly used in Korean painted cultural heritages. However, due to the lack of detailed records on the maintenance of the murals of Sungseonjeon, more specific interpretations cannot be drawn in this study, that is, the synthetic pigments used during reconstruction in 1878 (Lee et al., 2020) or the repair work carried out in 1987 (Baek, 1989) could not be distinguished.

Nevertheless, to improve cultural heritage site surveys, we emphasize the role of non-destructive analytical instruments in providing more detailed mineralogical traces compared to conventional analysis techniques. The application of these analysis methods to various cultural heritages with more detailed historical records compared to those of the current study will elucidate the use of earth materials and technology by our ancestors.

## 4. CONCLUSIONS

This study accurately identified mineral pigments in the wall paintings of the Sungseonjeon Hall in the royal tomb of King Suro, Historic Site No. 73, in Gimhae, South Korea through the complementary application of non-invasive analyses such as

PXRF, Raman, and ND-XRD. The results of this study suggest the possibility of improving non-destructive in situ investigation methods for cultural heritage in the future.

In the wall paintings produced at the time Sungseonjeon Hall was built or prior to the 18th century (group O), talc, minium with cinnabar, atacamite with botallackite, and lazurite were detected in white, red, green, and blue specimens, respectively, confirming the use of traditional mineral pigments dating back to ancient times. In contrast, in the wall paintings added later (group N), crocoite-based pigments were found to have been used in yellow specimens, along with anatase, minium, lavendulan with cornwallite, and lazurite. These results provide significant evidence for the cultural history of traditional mineral pigments that have been used since ancient times to produce wall paintings, as well as synthetic pigments such as titanium white, emerald green, and chrome yellow. In particular, according to the history of Korean painting cultural heritages, traces of modern painting materials indicate that the production period of the Group N wall paintings is at least after the end of the Joseon Dynasty (the late 19th century to the beginning of the 20th century).

## ACKNOWLEDGMENTS

This study was carried out with the support of the Cultural Heritage Research and Development (R&D) project of the National Research Institute of Cultural Heritage of the Cultural Heritage Administration. We are grateful for specimens and images of wall paintings from Gimhae City Hall and Sungseonjeon Hall.

## REFERENCES

- Abe, Y., Nakai, I., Takahashi, K., Kawai, N., and Yoshimura, S., 2010, On-site analysis of archaeological artifacts excavated from the site on the outcrop at Northwest Saqqara, Egypt, by using a newly developed portable fluorescence spectrometer and diffractometer. *Analytical and Bioanalytical Chemistry*, 395, 1987–1996. <https://doi.org/10.1007/s00216-009-3141-x>
- Ahn, J.Y., Kim, S.Y., and Cheon, J.H., 2014, A study in pigment analysis and original mounting of the decorative painting at court. *Journal of Conservation Science*, 30, 39–53. (in Korean with English abstract) <https://doi.org/10.12654/JCS.2014.30.1.05>
- Ahn, Y.B., Yoo, J.H., Choie, M.J., and Lee, M.S., 2020, Accuracy assessment and classification of surface contaminants of stone cultural heritages using hyperspectral image – focusing on stone Buddhas in four directions at Gulbuls Temple site, Gyeongju. *Journal of Conservation Science*, 36, 73–81. (in Korean with English abstract) <https://doi.org/10.12654/JCS.2020.36.2.01>
- Alberghina, M.F., Germinario, C., Bartolozzi, G., Bracci, S., Grifa, C., Izzo, F., Russa, M.F., Magrini, D., Massa, E., Mercurio, M., Nardo, V.M., Oddo, M.E., Pagnotta, S., Pelagotti, A., Ponterio, R.C., Ricci, P., Rovella, N., Ruffolo, S.A., Schiavone, S., Spagnuolo, A., Vetromile, C., Zuchtriegel, G., and Lubritto, C., 2020, Non-invasive characterization of the pigment's palette used on the painted tomb slabs at Paestum archaeological site. *IOP Conference Series: Materials Science and Engineering*, Volume 949, Oct. 14–16. <https://doi.org/10.1088/1757-899X/949/1/012002>
- Baek, C.G., 1989, Detachment, transfer, and conservation of the wall painting of Sungseonjeon in Royal Tomb of King Suro, Gimhae, Korea. *MUNHWAJAE Korean Journal of Cultural Heritage Studies*, 22, 175–203. (in Korean)
- Ballirano, P. and Maras, A., 2006, Mineralogical characterization of the blue pigment of Michelangelo's fresco "The Last Judgment." *American Mineralogist*, 91, 997–1005. <https://doi.org/10.2138/am.2006.2117>
- Barnett, J.R., Miller, S., and Pearce, E., 2006, Colour and art: a brief history of pigments. *Optics and Laser Technology*, 38, 445–453. <https://doi.org/10.1016/j.optlastec.2005.06.005>
- Bell, I.M., Clark, R.J., and Gibbs, P.J., 1997, Raman spectroscopic library of natural and synthetic pigments (pre- ≈ 1850 AD). *Spectrochimica Acta Part A: Molecular and Biomolecular Spectroscopy*, 53, 2159–2179. [https://doi.org/10.1016/S1386-1425\(97\)00140-6](https://doi.org/10.1016/S1386-1425(97)00140-6)
- Bertolotti, G., Bersani, D., Lottici, P.P., Alesiani, M., Malcherek, T., and Schlüter, J., 2011, Micro-Raman study of copper hydroxychlorides and other corrosion products of bronze samples mimicking archaeological coins. *Analytical and Bioanalytical Chemistry*, 402, 1451–1457. <https://doi.org/10.1007/s00216-011-5268-9>
- Bicchieri, M., 2014, The purple Codex Rossanensis: spectroscopic characterisation and first evidence of the use of the elderberry lake in a sixth century manuscript. *Environmental Science and Pollution Research*, 21, 14146–14157. <https://doi.org/10.1007/s11356-014-3341-6>
- Bowen, A.W., 1991, The importance of X-ray diffraction in the non-destructive characterisation of high-strength aluminium alloys. In: Ruud, C.O., Bussière, J.F., and Green, R.E. (eds.), *Nondestructive Characterization of Materials IV*. Springer, Boston, p. 247–257. [https://doi.org/10.1007/978-1-4899-0670-0\\_30](https://doi.org/10.1007/978-1-4899-0670-0_30)
- Caggiani, M.C., Cosentino, A., and Mangone, A., 2016, Pigments Checker version 3.0, a handy set for conservation scientists: a free online Raman spectra database. *Microchemical Journal*, 129, 123–132. <https://doi.org/10.1016/j.microc.2016.06.020>
- Čermáková, Z., Bezdička, P., Němec, I., Hradilová, J., Šrein, V., Blažek, J., and Hradil, D., 2015, Naturally irradiated fluorite as a historic violet pigment: Raman spectroscopic and X-ray diffraction study. *Journal of Raman Spectroscopy*, 46, 236–243. <https://doi.org/10.1002/jrs.4627>
- Chiari, G., 2008, Saving art in situ. *Nature*, 453, 159. <https://doi.org/10.1038/453159a>
- Chun, Y.G. and Lee, C.H., 2011, Pigment analysis for wall paintings according to verification of penetration depth for X-ray: SSanggyesa Daeungeon (main hall of Ssanggyesa temple) in Nonsan. *Journal of Conservation Science*, 27, 269–276. (in Korean with English abstract)
- Chun, Y.G., Lee, M.S., Kim, Y.R., Lee, M.H., Choi, M.J., and Choi, K.H., 2015, Utilization of hyperspectral image analysis for monitoring of Stone Cultural Heritages. *Journal of Conservation Science*, 31, 395–402. (in Korean with English abstract) <https://doi.org/10.12654/JCS.2015.31.4.07>

- Clair, K. St., 2016, *The Secret Lives of Colour*. John Murray, London, 319 p.
- Coccatto, A., Bersani, D., Coudray, A., Sanyova, J., Moens, L., and Vandenberghe, P., 2016, Raman spectroscopy of green minerals and reaction products with an application in Cultural Heritage research. *Journal of Raman Spectroscopy*, 47, 1429–1443. <https://doi.org/10.1002/jrs.4956>
- Culka, A. and Jehlička, J., 2019, A database of Raman spectra of precious gemstones and minerals used as cut gems obtained using portable sequentially shifted excitation Raman spectrometer. *Journal of Raman Spectroscopy*, 50, 262–280. <https://doi.org/10.1002/jrs.5504>
- Delaney, J.K., Dooley, K.A., van Loon, A., and Vandivere, A., 2020, Mapping the pigment distribution of Vermeer's *Girl with a Pearl Earring*. *Heritage Science*, 8, 4. <https://doi.org/10.1186/s40494-019-0348-9>
- Eastaugh, N., Walsh, V., Chaplin, T., and Siddall, R., 2004, *The Pigment Compendium: A Dictionary of Historical Pigments*. Elsevier Butterworth-Heinemann, Oxford, 416 p.
- Edwards, H.G.M., Farwell, D.W., Newton, E.M., and Perez, F.R., 1999, Minium; FT-Raman non-destructive analysis applied to an historical controversy. *Analyst*, 124, 1323–1326. <https://doi.org/10.1039/A904083H>
- Edwards, H.G.M., Jorge Villar, S.E., and Eremin, K.A., 2004, Raman spectroscopic analysis of pigments from dynastic Egyptian funerary artefacts. *Journal of Raman Spectroscopy*, 35, 786–795. <https://doi.org/10.1002/jrs.1193>
- El-Deen, S.E., Hashem, A.M., Abdel Ghany, A.E., Indris, S., Ehrenberg, H., Mauger, A., and Julien, C.M., 2018, Anatase TiO<sub>2</sub> nanoparticles for lithium-ion batteries. *Ionics*, 24, 2925–2934. <https://doi.org/10.1007/s11581-017-2425-y>
- Fan, X., Wang, Q., and Wang, Y., 2020, Non-destructive in situ Raman spectroscopic investigation of corrosion products on the bronze dagger-axes from Yujiaba site in Chongqing, China. *Archaeological and Anthropological Sciences*, 12, 90. <https://doi.org/10.1007/s12520-020-01042-0>
- Frison, G. and Brun, G., 2016, Lapis lazuli, lazurite, ultramarine 'blue', and the colour term 'azure' up to the 13th century. *Journal of the International Colour Association*, 16, 41–55.
- Garcia-Guinea, J., Tormo, L., Ordoñez, A.R., and Garcia-Moreno, O., 2013, Non-destructive analyses on a meteorite fragment that fell in the Madrid city centre in 1896. *Talanta*, 114, 152–159. <https://doi.org/10.1016/j.talanta.2013.03.070>
- Geldof, M., van der Werf, I.D., and Haswell, R., 2019, The examination of Van Gogh's chrome yellow pigments in 'Field with Irises near Arles' using quantitative SEM-WDX. *Heritage Science*, 7, 100. <https://doi.org/10.1186/s40494-019-0341-3>
- Gettens, R.J. and Stout, G.L., 1942, *Painting Materials: A Short Encyclopaedia*. D. Van Nostrand Company, New York, 333 p.
- Gliozzo, E. and Ionescu, C., 2022, Pigments—Lead-based whites, reds, yellows and oranges and their alteration phases. *Archaeological and Anthropological Sciences*, 14, 17. <https://doi.org/10.1007/s12520-021-01407-z>
- Gutiérrez-Neira, P.C., Agulló-Rueda, F., Climent-Font, A., and Garrido, C., 2013, Raman spectroscopy analysis of pigments on Diego Velázquez paintings. *Vibrational Spectroscopy*, 69, 13–20. <https://doi.org/10.1016/J.VIBSPEC.2013.09.007>
- Ha, J.W. and Lee, S.J., 2015, Identification of natural inorganic pigments used on 18th century Korean traditional mural paintings by using a portable X-ray fluorescence. *Journal of Industrial and Engineering Chemistry*, 28, 328–333. <https://doi.org/10.1016/j.jiec.2015.03.011>
- Hansford, G.M., 2013, X-ray diffraction without sample preparation: proof-of-principle experiments. *Nuclear Instruments and Methods in Physics Research Section A: Accelerators, Spectrometers, Detectors and Associated Equipment*, 728, 102–106. <https://doi.org/10.1016/j.nima.2013.06.065>
- Hansford, G.M., Turner, S.M.R., Degryse, P., and Shorland, A.J., 2017, High-resolution X-ray diffraction with no sample preparation. *Acta Crystallographica Section A*, A73, 293–311. <https://doi.org/10.1107/S2053273317008592>
- Hazen, R., Golden, J., Downs, R.T., Hystad, G., Grew, E.S., Azzolini, D., and Sverjensky, D., 2012, Mercury (Hg) mineral evolution: a mineralogical record of supercontinent assembly, changing ocean geochemistry, and the emerging terrestrial biosphere. *American Mineralogist*, 97, 1013–1042. <http://dx.doi.org/10.2138/am.2012.3922>
- Hoffman, D.L., Angelucci, D.E., Villaverde, V., Zapata, J., and Zilhão, J., 2018a, Symbolic use of marine shells and mineral pigments by Iberian Neandertals 115,000 years ago. *Science Advances*, 4, eaar5255. <https://doi.org/10.1126/sciadv.aar5255>
- Hoffman, D.L., Standish, C.D., Garcia-Diez, M., Pettitt, P.B., Milton, J.A., Zilhão, J., Alcolea-González, J.J., Cantalejo-Duarte, P., Colado, H., De Balbín, R., Lorblanchet, M., Ramos-Munoz, J., Weninger, G.-Ch., and Pike, A.W.G., 2018b, U-Th dating of carbonate crusts reveals Neandertal origin of Iberian cave art. *Science*, 359, 912–915. <http://science.org/doi/10.1126/science.aap7778>
- Holakooei, P. and Karimy, A.-H., 2015, Early Islamic pigments used at the Masjid-i Jame of Fahraj, Iran: a possible use of black plattnerite. *Journal of Archaeological Science*, 54, 217–227. <https://doi.org/10.1016/j.jas.2014.12.001>
- Hong, J.O. and Lee, J.J., 2013, Analysis of dancheong pigments at the Nahanjeon Songkwangsa Temple, Wanju. *Conservation Studies*, 34, 102–108. (in Korean with English abstract)
- Hradil, D., Hradilová, J., Bezdička, P., Švarcová, S., Čermáková, Z., Košarová, V., and Němec, I., 2014, Crocoite PbCrO<sub>4</sub> and mimetite Pb<sub>2</sub>(AsO<sub>4</sub>)<sub>3</sub>Cl: rare minerals in highly degraded mediaeval murals in Northern Bohemia. *Journal of Raman Spectroscopy*, 45, 848–858. <https://doi.org/10.1002/jrs.4556>
- Jeong, J.M., 2001, *Color and Drawing of Traditional Korean Painting. Hakgojae*, Seoul, 259 p. (in Korean)
- Keim, M. and Markl, G., 2015, Weathering of galena: mineralogical processes, hydrogeochemical fluid path modeling, and estimation of the growth rate of pyromorphite. *American Mineralogist*, 100, 1584–1594. <https://doi.org/10.2138/am-2015-5183>
- Kendrick, E., Dann, S.E., Hellgardt, K., and Weller, M.T., 2004, The effect of different precursors on the synthesis of ultramarine blue using a modified test furnace. *Studies in Surface Science and Catalysis*, 154, 3059–3066. [https://doi.org/10.1016/S0167-2991\(04\)80592-5](https://doi.org/10.1016/S0167-2991(04)80592-5)
- Kim, Y.S., Lee, S.J., Choi, I.S., Jin, B.H., and Lee, H.S., 2014, Study on the material characteristic of Baekeuikwaneum (the white-robed Buddhist goddess of mercy) wall-painting of Bogwangmyungjun in Wibongsa, Wanju. *Journal of Conservation Science*, 30, 55–65.

- (in Korean with English abstract)
- Klisińska-Kopacz, A., Łydzba-Kopczyńska, B., Czarnecka, M., Koźlecki, T., del Hoyo Mélendez, J., Mendys, A., Kłosowska-Klechowska, A., Obarzanowski, M., and Frączek, P., 2019, Raman spectroscopy as a powerful technique for the identification of polymers used in cast sculptures from museum collections. *Journal of Raman Spectroscopy*, 50, 213–221. <https://doi.org/10.1002/jrs.5407>
- Kostomitsopoulou Marketou, A., Andriulo, F., Steindal, C., and Handberg, S., 2020, Egyptian blue pellets from the first century BCE workshop of Kos (Greece): microanalytical investigation by optical microscopy, scanning electron microscopy-X-ray energy dispersive spectroscopy and micro-Raman spectroscopy. *Minerals*, 10, 1063. <https://doi.org/10.3390/min10121063>
- Lee, H.H., Park, J.H., Hong, J.O., Han, M.S., Seo, M.S., and Heo, J.S., 2012, The analytical study of pigments on four guardian statues in Song-gwang Buddhist Temple in Suncheon – focusing on pigments of Virupaksha. *MUNHWAJAE Korean Journal of Cultural Heritage Studies*, 45, 122–147. (in Korean with English abstract) <https://doi.org/10.22755/kjchs.2012.45.1.122>
- Lee, J.J., Ahn, J.Y., Yoo, Y.M., Lee, K.M., and Han, M.S., 2017, Diagnosis of coloration status and scientific analysis for pigments to used large Buddhist painting (Gwaebultaeng) in Tongdosa Temple. *Journal of Conservation Science*, 33, 431–442. (in Korean with English abstract) <https://doi.org/10.12654/JCS.2017.33.6.03>
- Lee, J.J., Han, M.S., Kwon, H.N., Lee, J.S., Yun, J.H., and Kwon, Y.M., 2019, A comparative study on characteristics of fabrics and coloring pigments of Buddhist paintings of Geumtapsa Temple and Manyeonsa Temple. *Journal of Buddhist Art*, 28, 523–546. (in Korean with English abstract)
- Lee, N.R., Yu, Y.G., and Lee, H.S., 2021, Study on the characteristics of materials and manufacturing techniques for the mural paintings in Daemunjeon at Ssanggyesa Temple, Jindo. *Journal of Conservation Science*, 37, 701–711. (in Korean with English abstract) <https://doi.org/10.12654/JCS.2021.37.6.09>
- Lee, S.M., Lee, S.H., and Roh, J.S., 2021, Analysis of activation process of carbon black based on structural parameters obtained by XRD Analysis. *Crystals*, 11, 153. <https://doi.org/10.3390/cryst11020153>
- Lee, S.M., Yoo, Y.E., Yoon, J.H., and Kim, Y.J., 2020, Investigation services on the value of national intangible cultural property of Sungseonjeon Rituals. Policy Research Service Report 76-5350145-000011-01, Gimhae City, South Korea, 198 p. (in Korean)
- Li, J., Tian, X., Xiao, X., Yang, F., and Zhao, F., 2022, Transforming cerussite to pyromorphite by immobilising Pb(II) using hydroxyapatite and *Pseudomonas rhodesiae*. *Chemosphere*, 287, 132235. <https://doi.org/10.1016/j.chemosphere.2021.132235>
- Li, Z., Wang, L., Chen, H., and Ma, Q., 2020, Degradation of emerald green: scientific studies on multi-polychrome Vairocana Statue in Dazu Rock Carvings, Chongqing, China. *Heritage Science*, 8, 64. <https://doi.org/10.1186/s40494-020-00410-2>
- Lubas, M., Jasinski, J.J., Sitarz, M., Kurpaska, L., Podsiad, P., and Jasinski, J.J., 2014, Raman spectroscopy of TiO<sub>2</sub> thin films formed by hybrid treatment for biomedical applications. *Spectrochimica Acta Part A: Molecular and Biomolecular Spectroscopy*, 133, 867–871. <https://doi.org/10.1016/j.saa.2014.05.045>
- Maneckí, M., Kwas'niak-Kominek, M., Majka, J., and Rakovan, J., 2020, Model of interface-coupled dissolution-precipitation mechanism of pseudomorphic replacement reaction in aqueous solutions based on the system of cerussite PbCO<sub>3</sub> – pyromorphite Pb<sub>5</sub>(PO<sub>4</sub>)<sub>3</sub>Cl. *Geochimica et Cosmochimica Acta*, 289, 1–13. <https://doi.org/10.1016/j.gca.2020.08.015>
- Martí, A.P., Zilhão, J., d'Errico, F., Cantalejo-Duarte, P., Domínguez-Bella, S., Fullola, J.M., Weniger, G.C., and Ramos-Muñoz, J., 2021, The symbolic role of the underground world among Middle Paleolithic Neanderthals. *Proceedings of the National Academy of Sciences of the United States of America*, 118, e2021495118. <https://doi.org/10.1073/pnas.2021495118>
- Marucci, G., Beeby, A., Parker, A.W., and Nicholson, C.E., 2018, Raman spectroscopic library of medieval pigments collected with five different wavelengths for investigation of illuminated manuscripts. *Analytical Methods*, 10, 1219–1236. <https://doi.org/10.1039/C8AY00016F>
- Merkaj, E. and Civici, N., 2020, Application of a portable XRF spectrometer for in-situ and nondestructive investigation of pigments in two 15th century icons. *Open Journal of Applied Sciences*, 10, 305–317. <https://doi.org/10.4236/ojapps.2020.106023>
- Miriello, D., Bloise, A., Crisci, G.M., De Luca, R., De Nigris, B., Martellone, A., Osanna, M., Pace, R., Pecci, A., and Ruggieri, N., 2018, Non-destructive multi-analytical approach to study the pigments of wall painting fragments reused in mortars from the archaeological site of Pompeii (Italy). *Minerals*, 8, 134. <https://doi.org/10.3390/min8040134>
- Moon, D.H., 2021, Mineralogical study on the raw materials of cultural properties; Interpretation and rediscovery. Ph.D. Thesis, Gyeong-sang National University, Jinju, South Korea, 107 p. (in Korean with English abstract)
- Moon, D.H. and Lee, M.S., 2019, Possibility about application and interpretation of surface nondestructive X-ray diffraction method for cultural heritage samples by material. *Journal of the Mineralogical Society of Korea*, 32, 287–301. (in Korean with English abstract)
- Moon, D.H., Lee, N.R., and Lee, E.W., 2021, Ancient pigments in Afrasiab murals: characterization by XRD, SEM, and Raman spectroscopy. *Minerals*, 11, 939. <https://doi.org/10.3390/min11090939>
- Mugnaini, S., Bagnoli, A., Bensi, P., Droghini, E., Scala, A., and Guasparri, G., 2006, Thirteenth century wall paintings under the Siena Cathedral (Italy). Mineralogical and petrographic study of materials, painting techniques and state of conservation. *Journal of Cultural Heritage*, 7, 171–185. <https://doi.org/10.1016/j.culher.2006.04.002>
- Nakai, I. and Abe, Y., 2012, Portable X-ray powder diffractometer for the analysis of art and archaeological materials. *Applied Physics A*, 106, 279–293. <https://doi.org/10.1007/s00339-011-6694-4>
- Nel, P., Lau, D., Hay, D., and Wright, N., 2006, Non-destructive micro-X-ray diffraction analysis of painted artefacts: determination of detection limits for the chromium oxide-zinc oxide matrix. *Nuclear Instruments and Methods in Physics Research Section B: Beam Interactions with Materials and Atoms*, 251, 489–495. <https://doi.org/10.1016/j.nimb.2006.07.003>
- Nord, A.G., Billström, K., Tronner, K., and Olausson, K.B., 2015, Lead isotope data for provenancing mediaeval pigments in Swedish mural paintings. *Journal of Cultural Heritage*, 16, 856–861. <https://doi.org/10.1016/j.culher.2015.02.009>
- Papliaka, Z.E., Philippidis, A., Siozos, P., Vakondiou, M., Melessanaki,

- K., and Anglos, D., 2016, A multi-technique approach, based on mobile/portable laser instruments, for the in situ pigment characterization of stone sculptures on the island of Crete dating from Venetian and Ottoman period. *Heritage Science*, 4, 15. <https://doi.org/10.1186/s40494-016-0085-2>
- Park, J.H., Jeong, H.Y., Go, I.H., Jeong, S.L., and Jo, A.H., 2015, A study on the physical properties of Seokrok and Noerok used as green pigment. *Journal of Conservation Science*, 31, 429–441. (in Korean with English abstract) <https://doi.org/10.12654/JCS.2015.31.4.10>
- Peng, W.G., Strauss, M., Pieper, T., and Kilian H.-G., 1993, X-ray diffraction and model calculation on carbon blacks. *Molecular Physics*, 80, 429–441. <https://doi.org/10.1080/00268979300102351>
- Pollard, A.M., Thomas, R.G., and Williams, P.A., 1989, Synthesis and stabilities of the basic copper(II) chlorides atacamite, paratacamite and botallackite. *Mineralogical Magazine*, 53, 557–563. <https://doi.org/10.1180/minmag.1989.053.373.06>
- Reiche, I., 2019, Mineral pigments: the colorful palette of nature. In: Artioli, G. and Oberti, R. (eds.), *The Contribution of Mineralogy to Cultural Heritage*. EMU Notes in Mineralogy Series, European Mineralogical Union, London, UK, 20, p. 283–322. <https://doi.org/10.1180/EMU-notes.207>
- Ribechini, E., Modugno, F., Pérez-Arantegui, J., and Colombini, M.P., 2011, Discovering the composition of ancient cosmetics and remedies: analytical techniques and materials. *Analytical and Bioanalytical Chemistry*, 401, 1727–1738. <https://doi.org/10.1007/s00216-011-5112-2>
- Riederer, J., 1974, Recently identified Egyptian pigments. *Archaeometry*, 16, 102–109. <https://doi.org/10.1111/j.1475-4754.1974.tb01098.x>
- Rodríguez, J., Montero-Ruiz, I., Hunt-Ortiz, M., and García-Pavón, E., 2020, Cinnabar provenance of Chalcolithic red pigments in the Iberian Peninsula: a lead isotope study. *Geoarchaeology*, 35, 871–882. <https://doi.org/10.1002/gea.21810>
- Rosi, F., Miliani, C., Borgia, I., Brunetti, B.G., and Sgamellotti, A., 2004, Identification of nineteenth century blue and green pigments by in situ X-ray fluorescence and micro-Raman spectroscopy. *Journal of Raman Spectroscopy*, 35, 610–615. <https://doi.org/10.1002/jrs.1180>
- Rousaki, A., Vázquez, C., Aldazábal, V., Bellelli, C., Carballido Calatayud, M., Hajduk, A., Vargas, E., Palacios, O., Vandenaabeele, P., and Moens, L., 2017, The first use of portable Raman instrumentation for the in situ study of prehistoric rock paintings in Patagonian sites. *Journal of Raman Spectroscopy*, 48, 1459–1467. <https://doi.org/10.1002/jrs.5107>
- Santos, H.C., Silva, T.F., Leite, A.R., Assis, R.F., Campos, P.H.O.V., Rizzutto, M.A., and Tabacniks, M.H., 2019, Characterization of a system that combines energy dispersive X-ray diffraction with X-ray fluorescence and its potential applications in archeometry. *Journal of Applied Physics*, 126, 044901. <https://doi.org/10.1063/1.5108746>
- Saviello, D., Di Gioia, A., Turenne, P.-I., Trabace, M., Giorgi, R., Mirabile, A., Baglioni, P., and Iacopino, D., 2019, Handheld surface-enhanced Raman scattering identification of dye chemical composition in felt-tip pen drawings. *Journal of Raman Spectroscopy*, 50, 222–231. <https://doi.org/10.1002/jrs.5411>
- Secco, M., Rainer, L., Graves, K., Heginbotham, A., Artioli, G., Piqué, F., and Angelini, I., 2021, Ochre-based pigments in the Tablinum of the House of the Bicentenary (Herculaneum, Italy) between decorative technology and natural disasters. *Minerals*, 11, 67. <https://doi.org/10.3390/min11010067>
- Seo, J.H., Cha, B.G., and Jung, H.S., 2011, Pigment analysis and conservation method of Avalokitesvara in Potalaka of Hyeondeungsa, Gapyeong. *Journal of Conservation Science*, 27, 223–229. (in Korean with English abstract)
- Shen, J. and Shen, Y., 2021, Identification of cinnabar existing in different objects using portable coupled XRF-XRD, laboratory-type XRD and micro-Raman spectroscopy: comparison of the techniques. *SN Applied Sciences*, 3, 866. <https://doi.org/10.1007/s42452-021-04858-0>
- Siddall, R., 2018, Mineral pigments in archaeology: their analysis and the range of available materials. *Minerals*, 8, 201. <https://doi.org/10.3390/min8050201>
- Song, Y.N., 2018, Materials characteristics of pigments on Dancheong in Joseon Dynasty. Ph.D. Thesis, Kongju National University, Gongju, South Korea, 276 p. (in Korean with English abstract)
- Tomasini, E.P., Gómez, B.A., Halac, E.B., Reinoso, M., Di Liscia, E., Siracusano, G., and Maier, M.S., 2015, Identification of carbon-based black pigments in four South American polychrome wooden sculptures by Raman microscopy. *Heritage Science*, 3, 19. <https://doi.org/10.1186/s40494-015-0049-y>
- Tomasini, E.P., Halac, E.B., Reinoso, M., Liscia, E.J., and Maier, M.S., 2012, Micro-Raman spectroscopy of carbon-based black pigments. *Journal of Raman Spectroscopy*, 43, 1671–1675. <https://doi.org/10.1002/jrs.4159>
- Tuschel, D., 2019, Raman spectroscopy and polymorphism. *Spectroscopy*, 34, 10–21.
- Venkatakrishnan, R., Senthilvelan, T., and Vijayakumar, T., 2017, Characterization of polyurethane coated aerospace aluminium alloy (7075) by DSC, XRD and adhesion test. *Journal of Applied Mechanical Engineering*, 6, 1000296. <https://doi.org/10.4172/2168-9873.1000296>
- Wagner, B., Donten, M.L., Donten, M., Bulska, E., Jackowska, A., and Sobucki, W., 2007, Analytical approach to the conservation of the ancient Egyptian manuscript “Bakai Book of the Dead”: a case study. *Microchimica Acta*, 159, 101–108. <https://doi.org/10.1007/s00604-007-0732-0>
- Wang, A., Freeman, J.J., and Jolliff, L., 2015, Understanding the Raman spectral features of phyllosilicates. *Journal of Raman Spectroscopy*, 46, 829–845. <https://doi.org/10.1002/jrs.4680>
- Watts, I., 2010, The pigments from Pinnacle Point Cave 13B, Western Cape, South Africa. *Journal of Human Evolution*, 59, 392–411. <https://doi.org/10.1016/j.jhevol.2010.07.006>
- Wu, X., Zhang, C., Goldberg, P., Cohen, D., Pan, Y., Arpin, T., and Bar-Yosef, O., 2012, Early pottery at 20,000 years ago in Xianrendong Cave, China. *Science*, 336, 1696–1700. <http://science.org/doi/10.1126/science.1218643>
- Yoo, Y.M., Han, M.S., and Lee, J.J., 2014, Species and characteristics of particles for traditional red and green pigments used in temples. *Journal of the Conservation Science for Cultural Properties*, 30, 365–372. (in Korean with English abstract) <https://doi.org/10.12654/JCS.2014.30.4.05>
- Zilhão, J., Angelucci, D.E., Badal-García, E., d’Errico, F., Daniel, F.,

Dayet, L., Douka, K., Higham, T.F.G., Martínez-Sánchez, M.J., Montes-Bernárdez, R., Murcia-Mascarós, S., Pérez-Sirvent, C., Roldán-García, C., Vanhaeren, M., Villaverde, V., Wood, R., and Zapata, J., 2010, Symbolic use of marine shells and mineral pigments by Iberian Neandertal. *Proceedings of the National Academy of Sciences*

of the United States of America, 107, 1023–1028. <https://doi.org/10.1073/pnas.0914088107>

**Publisher's Note** Springer Nature remains neutral with regard to jurisdictional claims in published maps and institutional affiliations.